

Mucoadhesive maleimide-functionalised liposomes for drug delivery to urinary bladder

Article

Accepted Version

Creative Commons: Attribution-Noncommercial-No Derivative Works 4.0

Kaldybekov, D., Tonglairoum, P., Opanasopit, P. and Khutoryanskiy, V. V. (2018) Mucoadhesive maleimide-functionalised liposomes for drug delivery to urinary bladder. *European Journal of Pharmaceutical Sciences*, 111. pp. 83-90. ISSN 0928-0987 doi:
<https://doi.org/10.1016/j.ejps.2017.09.039> Available at
<http://centaur.reading.ac.uk/72941/>

It is advisable to refer to the publisher's version if you intend to cite from the work. See [Guidance on citing](#).

Published version at: <http://www.sciencedirect.com/science/article/pii/S0928098717305316>

To link to this article DOI: <http://dx.doi.org/10.1016/j.ejps.2017.09.039>

Publisher: Elsevier

All outputs in CentAUR are protected by Intellectual Property Rights law, including copyright law. Copyright and IPR is retained by the creators or other

copyright holders. Terms and conditions for use of this material are defined in the [End User Agreement](#).

www.reading.ac.uk/centaur

CentAUR

Central Archive at the University of Reading

Reading's research outputs online

Mucoadhesive maleimide-functionalised liposomes for drug delivery to urinary bladder

Daulet B. Kaldybekov^{a,b}, Prasopchai Tonglairoum^{a,c}, Praneet Opanasopit^c, Vitaliy V. Khutoryanskiy^{a,*}

^a School of Pharmacy, University of Reading, Whiteknights, Reading, RG6 6AD, United Kingdom

^b Faculty of Chemistry and Chemical Technology, Al-Farabi Kazakh National University, Almaty, 050040, Kazakhstan

^c Pharmaceutical Development of Green Innovations Group, Faculty of Pharmacy, Silpakorn University, Nakhon Pathom, 73000, Thailand

*Corresponding author:

Prof V.V. Khutoryanskiy

Postal address: School of Pharmacy, University of Reading, Whiteknights, Reading, RG6 6AD, United Kingdom

E-mail address: v.khutoryanskiy@reading.ac.uk

Telephone: +44(0)1183786119

Fax: +44 (0) 118 378 4703

Abstract

Intravesical drug administration is used to deliver chemotherapeutic agents via a catheter to treat bladder cancer. The major limitation of this treatment is poor retention of the drug in the bladder due to periodic urine voiding. In this work, maleimide-functionalised PEGylated liposomes (PEG-Mal) were explored as mucoadhesive vehicles for drug delivery to the urinary bladder. The retention of these liposomes on freshly excised porcine bladder mucosa *in vitro* was compared with conventional liposomes, PEGylated liposomes, two controls (dextran and chitosan), and evaluated through Wash Out₅₀ (WO₅₀) values. PEG-Mal liposomes exhibited greater retention on mucosal surfaces compared to other liposomes. The penetration abilities of conventional, PEG-Mal-functionalised and PEGylated liposomal dispersions with encapsulated fluorescein sodium into the bladder mucosa *ex vivo* were assessed using a fluorescence microscopy technique. PEGylated liposomes were found to be more mucosa-penetrating compared to other liposomes. All liposomes were loaded with fluorescein sodium salt as a model drug and the *in vitro* release kinetics was evaluated. Longer drug release was observed from PEG-Mal liposomes.

34 *Keywords: liposomes, urinary bladder, intravesical drug delivery, mucoadhesion, mucus penetration,*
35 *wash out₅₀ (WO₅₀)*

36

37 **1. Introduction**

38 Bladder cancer (BC) is caused by uncontrolled growth of tumour cells in the urinary bladder. It
39 has the 9th highest incidence globally, with an estimated 430,000 newly diagnosed cases in 2012
40 (Stewart and Wild, 2014). The prevalence of this malignancy of the genitourinary tract tends to
41 increase with economic development and males are more likely to develop this condition than females
42 (Torre et al., 2015). The most common type of BC is transitional cell carcinomas that comprise over
43 90% of tumours, while squamous cell carcinomas and adenocarcinomas represent about 5% and 1% of
44 the reported cases, respectively.

45 Intravesical drug delivery (IDD) is a direct administration of therapeutic agents into the bladder
46 via insertion of a urethral catheter (Au et al., 2001; Malmström, 2003; Kolawole et al., 2017). This
47 allows localised treatment, minimises adverse effects and improves the exposure of the diseased tissues
48 to therapeutic agents. Also, the oral route of the drug intake is undesirable in the therapy of BC due to
49 absorption, metabolism and renal excretion, resulting in poor drug bioavailability in the bladder.

50 IDD has intrinsic limitations related to the substantial chemotherapy dilution and wash out due to
51 urinary voiding, low permeability of the urothelium, and intermittent catheterisations (GuhaSarkar and
52 Banerjee, 2010). Additionally, the procedure is relatively unpleasant for the patients and may cause
53 inflammatory reactions and infections. To counteract the limitations associated with low drug
54 permeability, mucoadhesive formulations offer great promise. The ability of mucoadhesive materials to
55 adhere to the bladder epithelium and withstand wash out effect could improve drug bioavailability by
56 prolonging the residence in the bladder. Mucoadhesive formulations for IDD must fulfill the following
57 criteria: the dosage form should have rapid and efficient adhesion to the bladder mucosa; must not
58 interfere with the normal physiology of the bladder; and should be able to stay adhered *in situ* for a
59 few hours even after urination (Tyagi et al., 2006).

60 A number of mucoadhesive formulations have been researched, including the use of hydrophilic
61 polymers of both natural and synthetic type, such as chitosan, carbomers and cellulose derivatives
62 (Hombach and Bernkop-Schnürch, 2010; Khutoryanskiy, 2011). The adherence of these polymers is
63 due to the ability to interact with mucin glycoproteins via non-covalent bonds such as hydrogen bonds,
64 electrostatic interactions and chain entanglements, diffusion and interpenetration (Khutoryanskiy,
65 2011; Davidovich-Pinhas and Bianco-Peled, 2014). In a comparative study, chitosan was found to

66 exhibit greater mucoadhesion to pig vesical mucosa compared to carboxymethylcellulose and
67 polycarbophyl, thus resulting in a slower drug release and longer residence time (Burjak et al., 2001).

68 In recent years, various chemical approaches have been used to improve mucoadhesive properties
69 of polymers by introducing specific functional groups such as thiols (Bernkop-Schnürch, 2005;
70 Davidovich-Pinhas et al., 2009; Cook et al., 2015), acrylates (Davidovich-Pinhas and Bianco-Peled,
71 2011; Brannigan and Khutoryanskiy, 2017), and catechols (Kim et al., 2015). Some studies reported
72 the use of chemically modified mucoadhesive materials for IDD to urinary bladder. Thiol-modified
73 chitosan nanoparticles (NPs) have been used for IDD in an *in vitro* study using porcine urinary bladder
74 (Barthelmes et al., 2011). It was found that chitosan functionalised with thiol groups demonstrated
75 superior mucoadhesion, greater stability and controlled release compared to the unmodified chitosan
76 NPs. In a different study, the retention of thiolated chitosan NPs on rat bladder mucosa *in vivo* was
77 approximately 170-fold greater compared to the polymer-free fluorescent marker (Barthelmes et al.,
78 2013). Mun et al. (2016) developed and evaluated the retention of thiolated and PEGylated silica NPs
79 on porcine urinary bladder mucosa *in vitro* through use of a novel Wash Out₅₀ (WO₅₀) quantitative
80 method. It was shown that the retention of these NPs on bladder mucosa depended on both their thiol
81 content and dimensions.

82 Recently we have demonstrated for the first time that polymers functionalised with maleimide
83 groups exhibit excellent mucoadhesive properties to conjunctival tissues *ex vivo* and the ability of these
84 materials to retain on mucosal tissues was comparable to well-known mucoadhesive chitosan
85 (Tonglairoum et al., 2016). This excellent mucoadhesive performance of maleimide-functionalised
86 polymers is due to their ability to form covalent linkages with thiol-groups present in mucins. More
87 recently, Shtenberg et al. (2017) reported the functionalisation of alginate with maleimide-terminated
88 polyethyleneglycol to achieve superior mucoadhesive properties towards porcine intestine mucosa.

89 Liposomes are microscopic vesicles composed of phospholipid bilayers with the size range from
90 30 nm up to several microns that have attracted a lot of interest over the past four decades as
91 pharmaceutical carriers. Conventional liposomes and liposomes coated with mucoadhesive polymers
92 previously were used for transmucosal drug delivery (Sasaki et al., 2013; Berginc et al., 2014;
93 Adamczak et al., 2017). Some liposome-based formulations were also reported for intravesical drug
94 delivery (Chuang et al., 2009, 2014; Kawamorita et al., 2016). Recently, Oswald et al. (2016) reported
95 the preparation and characterisation of maleimide-functionalised liposomes; however they did not
96 demonstrate any application of these systems for drug delivery.

97 In this study, we explored the mucoadhesive properties of maleimide-functionalised liposomes
98 and compared their retention on urinary bladder mucosa with conventional liposomes and PEGylated

99 liposomes. We also have studied the physicochemical properties of different liposomes, their
100 penetration into the bladder mucosa and drug release profiles.

101

102 **2. Materials and methods**

103 **2.1. Materials**

104 Soybean L-alpha-phosphatidylcholine (PC) was purchased from Alfa Aesar (Heysham, UK). [N-
105 (carbonyl-methoxypolyethylene glycol-2000)-1,2-distearoyl-sn-glycero-3-phosphoethanol-amine,
106 sodium salt] (MPEG₂₀₀₀-DSPE) was a generous gift from Lipoid GmbH (Ludwigshafen, Germany).
107 1,2-distearoyl-sn-glycero-3-phosphoethanolamine-N-[maleimide(polyethylene glycol)-2000]
108 ammonium salt (PEG₂₀₀₀-DSPE-Mal) was purchased from Avanti Polar Lipids (Alabaster, USA).
109 Cholesterol (CHO), chitosan (low molecular weight; Mw 62.3 kDa, PDI 3.42 as reported by Symonds
110 et al (2016)), fluorescein isothiocyanate dextran (FITC-dextran, Mw 3000-5000 Da), fluorescein
111 isothiocyanate (FITC) and fluorescein sodium salt (NaFI) were purchased from Sigma Aldrich
112 (Gillingham, UK). All other chemicals were of analytical grade and were used as received.

113 Phosphate-buffered saline (PBS) was composed of 8.0 g NaCl, 0.2 g KCl, 1.44 g Na₂HPO₄ and
114 0.24 g KH₂PO₄ (pH 7.4). The buffer solution was made with deionised water (total volume 1000 mL).

115

116 **2.2. Preparation of liposomes**

117 The liposomal formulations containing fixed amounts of PC, CHO and PEGylated lipids at molar
118 ratios of 10:2:0 and 10:2:3 mM (Table 1) were prepared using thin film hydration and sonication
119 method (Rangsimawong et al., 2016). In brief, a mixture of PC, CHO and PEGylated lipids dissolved
120 in chloroform-methanol (2:1, v/v) in test tubes. The organic solvent was evaporated under a stream of
121 nitrogen and a thin film of lipid was formed inside the test tubes. The test tubes were then placed under
122 vacuum at least 6 h to remove any residual solvent. Then, solution of NaFI in PBS (pH 7.4) was added
123 to the dried lipid films to generate hydrated liposome vesicles and the tubes were left for 1 h at room
124 temperature. The tubes were vortex-mixed vigorously for 30 min and these liposome dispersions were
125 then sonicated in a sonication bath (FS200b, Decon Laboratories Ltd., UK) for 30 min to reduce the
126 size of the liposomes. Excess lipids were separated from the vesicle formulations by centrifugation at
127 14000 rpm (8765 × g) at 4 °C for 30 min. The supernatants were collected and stored in a fridge
128 overnight prior to characterisation.

129

130 **2.3. Synthesis of fluorescently-labelled chitosan**

131 FITC-chitosan was synthesised according to the procedure described previously (Cook et al.,
132 2011; Symonds et al., 2016). Briefly, 1 g of chitosan was dissolved in 100 mL of acetic acid (0.1 M)
133 and left stirring overnight. 100 mg of FITC was dissolved in 50 mL of methanol and subsequently was
134 added to the chitosan solution and stirred for 3 h in the dark at room temperature. The modified
135 chitosan was then precipitated in 1 L of 0.1 M sodium hydroxide and filtered. The resulting product
136 was redissolved and purified by dialysis against deionised water in the dark to remove any unreacted
137 FITC before lyophilisation. FITC-chitosan was kept wrapped in aluminum foil to avoid exposure to
138 light and stored in a fridge for further use.

139

140 **2.4. Particle size and zeta potential analysis**

141 The size of liposomes, their polydispersity index (PDI) and zeta potential values were determined
142 using dynamic light scattering (DLS) with a Zetasizer Nano-ZS (Malvern Instruments, UK). Each
143 formulation was diluted 100-fold with ultrapure water. A typical liposome refractive index of 1.45 and
144 absorbance of 0.1 were used in all measurements. Each sample was analysed three times at 25 °C and
145 the mean \pm standard deviation values were calculated.

146

147 **2.5. Transmission electron microscopy**

148 TEM images were generated using a JEOL 2100Plus TEM operating at an acceleration voltage of
149 200kV. Specimens were prepared by pipetting a drop of liposome suspension diluted with water (about
150 5 mg/mL) onto a parafilm. A glow-discharged holey carbon film-coated 400-mesh copper grid was
151 then placed onto the drop with “carbon” side and left in contact with the sample for 1 min. The excess
152 solution was removed by blotting with a filter paper. The grid was washed by touching its surface with
153 sample side down on drop of deionised water on parafilm for 1 min and then blotted dry with a filter
154 paper. A drop of 1% (w/v) uranyl acetate (UA) solution was applied on parafilm and the grid remained
155 in contact with UA for 30 sec (PEG-Mal liposomes were stained for 5 sec, which provided better
156 quality of TEM images). The excess stain was removed by dabbing similarly and the sample was left to
157 dry in air prior to TEM characterisation.

158

159 **2.6. Encapsulation efficacy and loading capacity**

160 The lipid nanocarrier dispersion (500 μ L) was placed in an ultrafiltration tube using an Amicon®
161 Ultra-0.5 Ultracel-3 centrifugal filter unit with a molecular weight cutoff of 3 kDa and centrifuged at 4
162 °C at 14000 rpm ($8765 \times g$) for 60 min. The filtrate was discarded, and 250 μ L of PBS was added
163 before further centrifugation at 4 °C at 14000 rpm ($8765 \times g$) for 40 min. This washing step was

164 repeated twice. The NaFI-loaded liposomes in the retentate were then disrupted with 200 μ L of
165 methanol and centrifuged at 4 $^{\circ}$ C at 14000 \times g for 10 min. The amount of free NaFI in the supernatants
166 was quantified using a Varian Cary Eclipse fluorescence spectrometer at $\lambda_{\text{excitation}}$ and $\lambda_{\text{emission}} = 460$
167 and 512 nm, respectively, and the encapsulation efficiency (%EE) and loading capacity (%LC) were
168 calculated using the following equations:

$$\%EE = \frac{C}{C_i} \times 100$$
$$\%LC = \frac{C}{\text{Lipid composition}} \times 100$$

171
172 where C is the amount of NaFI entrapped in the liposomes, and C_i is the initial amount of NaFI.

173
174 A calibration curve used to calculate the encapsulation efficacy and loading capacity can be found in
175 Supplementary Information (Fig S1).

176

177 **2.7. Preparation of artificial urine solution**

178 Artificial urine solution was prepared according to the previously reported procedure
179 (Chutipongtanate and Thongboonkerd, 2010). The following components were dissolved in deionised
180 water by stirring for 6 h at room temperature, before making the total volume to 2000 mL: urea (24.27
181 g), uric acid (0.34 g), creatinine (0.90 g), $\text{Na}_3\text{C}_6\text{H}_5\text{O}_7 \cdot 2\text{H}_2\text{O}$ (2.97 g), NaCl (6.34 g), KCl (4.50 g),
182 NH_4Cl (1.61 g), $\text{CaCl}_2 \cdot 2\text{H}_2\text{O}$ (0.67 g), $\text{MgSO}_4 \cdot 7\text{H}_2\text{O}$ (1.00 g), NaHCO_3 (0.34 g), $\text{Na}_2\text{C}_2\text{O}_4$ (0.03 g),
183 Na_2SO_4 (2.58 g), $\text{NaH}_2\text{PO}_4 \cdot \text{H}_2\text{O}$ (1.00 g), and Na_2HPO_4 (0.11 g). The artificial urine solution (pH 6.4)
184 was kept at 37 $^{\circ}$ C throughout the experiments.

185

186 **2.8. *In vitro* retention studies on porcine urinary bladder**

187 The retention of the liposomes on porcine urinary bladder tissues were determined using a
188 protocol slightly modified from Mun et al. (2016). Porcine bladder tissues were received from P.C.
189 Turner Abattoirs (Farnborough, UK), immediately after animal slaughter, packed with dry ice and
190 transported in a polystyrene container. The tissues were defrosted upon arrival and carefully excised to
191 yield approximately 2 \times 3 cm sections, avoiding contact with the internal mucosa, which were then
192 used in the experiments. The dissected bladder tissue was mounted on a glass slide with mucosal side
193 facing upward and rinsed with 3 mL of AU solution. Experiments were performed with the bladder
194 tissues maintained at 37 $^{\circ}$ C in an incubator. Aliquots from NaFI-loaded liposome stock solutions were

195 withdrawn and diluted 1:1 with PBS (2.3 mg/mL), and aqueous solutions of FITC-chitosan (0.5 mg/mL
196 in 0.5% acetic acid) and FITC-dextran (0.5 mg/mL in deionised H₂O) were prepared. The pH of FITC-
197 chitosan solution was adjusted to pH 6 with 1% NaOH. An aliquot (20 µL) of either NaFI-loaded lipid
198 nanocarrier dispersions or polymers (controls) was pipetted onto a mucosal surface and irrigated with
199 AU solution at a flow rate of 2 mL/min using a syringe pump (total washing time was 50 min).
200 Fluorescence images of whole tissue were taken using a Leica MZ10F stereo-microscope (Leica
201 Microsystems, UK) with Leica DFC3000G digital camera at 0.8 × magnification with 20 ms exposure
202 time, fitted with a GFP filter. The microscopy images were then analysed with ImageJ software by
203 measuring the pixel intensity after each wash. The pixel intensity of the blank samples (bladder mucosa
204 without test material) were subtracted from each measurement. Each experiment was conducted in
205 triplicate.

206 Evaluation of retention of formulations on the mucosa *in vitro* was quantified through WO₅₀
207 values, which represent the volume of a biological fluid necessary to wash out 50% of a mucoadhesive
208 formulation from a substrate (Mun et al., 2016). WO₅₀ values of test materials were calculated via
209 extrapolation of the wash-off profiles to 50% using polynomial fitting.

210

211 **2.9. Mucosal penetration**

212 The mucosal permeation study was carried out as described in Mansfield et al. (2016) using
213 freshly excised porcine bladder tissues. NaFI-loaded liposome solutions were diluted 1:1 with PBS.
214 Aliquots (100 µL) of NaFI-loaded liposomes were deposited onto 2 × 2 cm² *ex vivo* bladder mucosa,
215 which were then placed on microscope slides. Deionised water was also pipetted as a blank control.
216 Samples were left to incubate for 15, 30, 45 and 60 min at 37 °C. Following each time point, tissue
217 pieces were placed with mucosal layer facing upward into a weighing boat (3.5 × 5.5 cm), half filled
218 with OCT, a cryoprotective embedding medium. They were then placed on dry ice, before being
219 completely embedded in OCT to conserve the liposome-loaded mucus membrane. Samples were then
220 left on dry ice for 3 h.

221 For sectioning, each sample was mounted onto a 22 mm standard metal sample holder using
222 OCT, and placed on dry ice for 30 min until completely frozen. Mucosal tissues were cryosectioned
223 transversely with a standard 189 × 27 × 10 mm blade at 5° to form 25 µm sections, placed onto
224 Superfrost® Plus charged microscope slides (Thermo Scientific, UK) and left to dry in air for 30 min
225 before being stored. All sections were cut upwards through the mucosal layer. All specimens were cut
226 using a Bright 5040 cryostat in a Bright Model PTF freezing chamber at -25 °C (Bright Instrument Co.
227 Ltd, UK).

228 Sections were placed under the Leica MZ10F fluorescence stereo-microscope and all images
229 taken with 160 ms exposure time through the GFP filter. 10 images were taken for each liposome type
230 from a separate section of tissue.

231 ImageJ software was used to evaluate penetration of the liposomes as described by Mansfield et
232 al. (2016). For each image, the background was subtracted, a line drawn across the mucosal barrier, and
233 the “plot profile” measured. This was repeated five times at random locations along the mucosal
234 surface for each image, giving 50 profiles for each sample. These profiles were then evaluated for
235 penetration of liposomes. This was achieved by measuring the widths of all peaks including the width
236 of the last peak as the urinary bladder mucosa is heavily folded. The mean values were calculated
237 following analysis of each profile. To determine penetration into mucosa the values obtained for the
238 blank tissue at each time point were then subtracted from the other values at the same time point.

239

240 **2.10. *In vitro* release of NaFI from liposomes**

241 The *in vitro* release of NaFI from liposomes was studied using a dialysis method adopted from
242 our previous publication (Tonglairoum et al., 2016). In brief, 2 mL of NaFI-loaded liposomes in AU
243 solution was transferred in a Pur-A-Lyzer™ Maxi 3500 dialysis membrane and immersed in 30 mL of
244 AU (pH 6.4) that was then shaken at 80 spm for 24 h at 37 °C. At regular intervals, aliquots (5 mL)
245 were withdrawn from the dialysate and replaced with fresh medium to maintain a constant volume. The
246 released NaFI was determined using fluorescence spectrometer ($\lambda_{\text{excitation}} = 460$ and $\lambda_{\text{emission}} = 512$ nm).
247 Fig 2S (Supplementary Information) shows the calibration curve used in these experiments. All release
248 experiments were conducted in triplicate.

249

250 **2.11. Statistical analysis**

251 Statistical analysis was performed using GraphPad Prism, v5.0. Mean values \pm standard
252 deviations were calculated and assessed for significance using one-way analysis of variance (ANOVA)
253 followed by Bonferoni *post hoc* test, where $p < 0.05$ was fixed as the statistical significance criterion.

254

255 **3. Results and discussion**

256 **3.1. Preparation and characterisation of liposomes**

257 Conventional, PEG-Mal and PEGylated liposomes were produced using standard thin film
258 hydration and sonication method and the amount of NaFI was kept equal in all preparations (Table 1).
259 The average mean diameter of all liposome preparations was $\sim 90 \pm 1$ nm and the polydispersity index
260 (PDI) was less than 0.23, which indicates the presence of a homogeneous liposomal population with a

261 narrow size distribution (Figure 1). The PDI is a measure of the size distribution and according to the
262 literature, liposomal formulation is considered to be homogenous if PDI is ≤ 0.30 (Verma et al., 2003).

263 Vesicles showing their zeta potential of less than -30 mV are believed to have excellent colloidal
264 stability and have the reduced number of bilayer membranes due to the electrostatic repulsion between
265 the charges of the same polarity. Furthermore, liposomal formulation with ≤ -30 mV would have higher
266 entrapment capacity because stronger zeta potential contributes to the increase in the unilamellar
267 vesicles (Sou, 2011; Kandzija and Khutoryanskiy, 2017). The physicochemical characteristics of
268 different liposomes are summarised in Table 2.

269 Many factors influence the encapsulation efficiency (%EE) and loading capacity (%LC) of
270 liposomes, including partition coefficient of the drug (logP), drug/liposome ratio, lipid composition,
271 bilayer rigidity, presence of charge, method of preparation, etc (Kulkarni et al., 1995; Nii and Ishii,
272 2005). According to the literature water-soluble drugs have, however, lower encapsulation in the
273 liposomes compared to their lipophilic counterparts (Kandzija and Khutoryanskiy, 2017); this depends
274 on the encapsulated aqueous volume. Since NaFI has a logP = -0.67 , we anticipated lower
275 encapsulation levels (Nii and Ishii, 2005).

276 NaFI was used as a model drug to demonstrate the potential use of liposomes for the application
277 in urinary bladder drug delivery. NaFI was loaded into the liposome formulations using standard thin
278 film method followed by sonication. It was found that conventional liposomes had the highest %EE
279 (53 ± 6 %), whereas PEG-Mal and PEGylated liposomes exhibited lower %EE of $25 \pm 2\%$ and $27 \pm 2\%$,
280 respectively (Table 2). It should be noted that %EE values determined in the present study are not fully
281 accurate as it was assumed that all 100 % of lipids used in the formulation were converted into
282 liposomes.

283 Transmission electron microscopy (TEM) can be used to evaluate the morphology and fine
284 structure of liposomes. The freeze-fracture electron microscopy and/or cryo-electron microscopy are
285 the optimal techniques to study the structure of rapidly frozen biological samples, membranes, proteins,
286 etc. by TEM, but the preparation of the specimens (cryofixation, fracturation, vitrification and the
287 following procedure of shading with evaporated platinum or gold, etc.) is complicated and requires
288 long time (Frederik and Hubert, 2005; Robenek and Severs, 2008; Thompson et al., 2016). In our
289 experience, negative staining is an easier and faster procedure. During negative staining liposomes are
290 treated with an electron dense material achieving reasonable contrast. In this work, we used uranyl
291 acetate that binds the phosphate group of phospholipids and has a limited penetration into the lipidic
292 bilayer (Harris, 1986).

293 TEM microphotographs of the produced liposomes are shown in Figure 2. TEM analysis revealed
294 the formation of a spherical and small unilamellar membrane for all liposome samples. Also, the
295 images show a population of homogeneous vesicles. It is also possible to see close bilayer structures
296 spaced by free internal structure. Furthermore, the negative staining of these liposomes confirms the
297 results obtained by the DLS analysis (Table 2). This observation is in agreement with the mechanism
298 that the negative charge on the membrane increases the unilamellar vesicles that have high entrapment
299 capacity. In addition, unlike conventional liposomes (Figure 2A), formation of aggregates can be
300 observed in PEG-Mal liposome formulations, which is likely to be due to the hydrophobic nature of
301 maleimide groups in their structure (Figure 2C).

302

303 **3.2. Mucoadhesion studies**

304 The retention properties of NaFI-loaded conventional, PEG-Mal and PEGylated liposomes on
305 porcine urinary bladder mucosa were assessed using a flow-through method with fluorescent detection
306 using the methodologies described in our previous publications (Irmukhametova et al., 2011; Storha et
307 al., 2013; Mun et al., 2016). Figure 3 shows exemplary fluorescent images of the retention of
308 conventional, PEG-Mal and PEGylated liposomal dispersions as well as two controls (chitosan and
309 dextran) on urinary bladder mucosa, washed with artificial urine (AU). FITC-chitosan and FITC-
310 dextran were used as a positive and negative controls, respectively (Mun et al., 2016; Tonglairoum et
311 al., 2016). However, it should be noted that there is a difference between the retention of FITC-
312 modified polymers and retention of free sodium fluorescein released from liposomes. After analysis of
313 the fluorescent images using ImageJ software, it was established that PEG-Mal liposomes exhibited
314 very good mucoadhesive properties, comparable to the retention of FITC-chitosan (Figure 4). It was
315 found that 32% of PEG-Mal liposomes remained on the bladder mucosa even after 50 min of washing
316 with a total AU volume of 100 mL. Moreover, the percentage retention of PEG-Mal liposomes was
317 found not to be significantly different from FITC-chitosan ($p > 0.05$), confirming that PEG-Mal
318 liposomes can also be adhered well on the bladder mucosa by forming covalent bonds with thiol groups
319 present in mucin layer of the bladder epithelium. Conventional liposomes had a significantly lower
320 retention capability compared to PEG-Mal liposomes ($p < 0.05$). It was found that approximately 18%
321 of conventional liposomes retained on the bladder epithelial mucosa after 100 mL of washing with AU.
322 These results confirm the mucoadhesive properties of maleimide-terminated PEGylated liposomes,
323 which could also be used as a potential mucoadhesive drug carrier. The mechanism of enhanced
324 mucoadhesion of maleimide-functionalised liposomes includes the formation of covalent linkages
325 between maleimide groups and thiols present on mucosal surfaces, as shown in Figure 5.

326 Mun et al. (2016) have described a novel quantitative method that allows evaluating and
327 comparing the retention efficiency of liquid formulations on mucosal surfaces through the use of Wash
328 Out₅₀ (WO₅₀) values, which represent the volume of a biological fluid required to wash out 50% of the
329 test mucoadhesive material from a substrate. In this work, WO₅₀ values were calculated by analysing
330 individual wash-off profiles and the results are summarised in Table 2. By comparing these values for
331 different liposomes used in this study, it is clear that the PEG-Mal liposomes have greater retention on
332 bladder mucosa (WO₅₀ = 48 mL, R²=0.9988), compared to conventional liposomes (WO₅₀ = 15 mL,
333 R²=0.9987), PEGylated liposomes (WO₅₀ = 24 mL, R²=0.9985) and non-mucoadhesive FITC-dextran
334 (WO₅₀ = 5 mL, R²=0.9903), but have weaker mucoadhesive ability than FITC-chitosan (WO₅₀ = 91
335 mL, R²=0.9970).

336

337 **3.3. Penetration into bladder mucosa**

338 In order to assess the penetration properties of NaFI-loaded conventional, PEG-Mal and
339 PEGylated liposomes through bladder mucosa, fluorescence microscopy was employed. The liposome
340 solutions were pipetted onto freshly excised porcine urinary bladder mucosa and were left in contact
341 with the tissues for 15, 30, 45 and 60 minutes and were then frozen and sectioned. Fluorescent images
342 were then collected and ImageJ software used to evaluate the penetration of liposomes. Figure 6
343 demonstrates that the PEG liposomes exhibit greater penetration ability ($p < 0.05$) than conventional
344 and PEG-Mal counterparts at all time points. The enhanced permeation performance of PEGylated
345 liposomes into the mucosa, compared to conventional liposomes is in excellent agreement with the
346 studies of PEGylated nanoparticles on different mucosal barriers (Wang et al., 2008; Mun et al., 2014).
347 PEG provides stealth properties to liposomes, making them less interactive with biological tissues that
348 facilitates their deeper penetration. This explains the greater diffusivity of PEGylated liposomes
349 through mucosal epithelium compared to conventional liposomes. The maleimide-functionalised PEG
350 liposomes are more mucoadhesive and will therefore form strong covalent bonds with thiols in mucosal
351 tissue and hence their penetration is slightly retarded (Figure 6). Representative exemplary fluorescent
352 images of the penetration of different liposomes through porcine bladder mucosa can be found in
353 Supplementary Information (Figure S3). Better penetration of PEG liposomes into bladder mucosa
354 could also provide some advantages for intravesical drug delivery; application of penetration enhancers
355 such as dimethylsulphoxide to facilitate deeper anticancer drug penetration has previously been reported
356 (Chen et al, 2003).

357

358 **3.4. In vitro release from liposomes**

359 The *in vitro* release studies for NaFI from conventional, PEG-Mal and PEGylated liposomes
360 were conducted in AU solution at 37 °C using a dialysis method and the cumulative release profiles are
361 shown in Figure 7. Conventional liposomes exhibited a rapid release of NaFI, which reaches saturation
362 after 2 h. PEGylated and PEG-Mal liposomes demonstrated a prolonged release, which reaches 95-100
363 % after 4 and 8 h, respectively. This difference is clearly related to the presence of PEG on liposomal
364 surfaces, which makes them more stable. A more prolonged release of a drug from PEG-Mal liposomes
365 provides an advantage as it will ensure better efficiency and will maintain a therapeutically-relevant
366 drug concentration in the bladder over a longer period of time following intravesical administration. A
367 delayed release of NaFI from liposomes could also improve model drug retention on the bladder.

368

369 **4. Conclusion**

370 Three liposomal formulations were evaluated in this work for their retention in the urinary
371 bladder, penetration into the mucosa and drug release *in vitro*. These formulations were prepared based
372 on conventional liposomes, PEGylated liposomes and liposomes decorated with maleimide-
373 functionalised PEG. The liposomes with maleimide groups exhibited superior *in vitro* retention on the
374 bladder tissue, which is related to their ability to form covalent bonds with thiols present in mucosal
375 tissue. PEGylated liposomes were found to have a greater ability to penetrate deeper into the mucosal
376 tissue due to the stealth character of PEG that facilitates mucus-penetrating properties.

377

378 **5. Acknowledgements**

379 The authors gratefully acknowledge the British Council Newton–Al-Farabi Partnership
380 Programme, the Researcher Links Post-doctoral Mobility Grant (216046068) for financial support and
381 for providing 2-years postdoctoral fellowship for Dr D.B. Kaldybekov at the University of Reading. Dr
382 Peter Harris is thanked for his help with TEM studies. The Chemical Analysis Facility (University of
383 Reading) is thanked for access to fluorescence spectrometer and TEM. P.C. Turner Abattoirs
384 (Farnborough, UK) is also acknowledged for providing pig bladders for experiments.

385

386 **Appendix A. Supplementary data**

387

388 **References**

389 Adamczak, M.I., Martinsen, Ø.G., Smistad, G., Hiorth, M., 2017. Polymer coated mucoadhesive
390 liposomes intended for the management of xerostomia. *Int. J. Pharm.* 527, 72–78.
391 Au, J.L., Badalament, R.A., Wientjes, M.G., Young, D.C., Warner, J.A., Venema, P.L., Pollifrone,

392 D.L., Harbrecht, J.D., Chin, J.L., Lerner, S.P., Miles, B.J., 2001. Methods to improve efficacy of
393 intravesical mitomycin C: results of a randomized phase III trial. *J. Natl. Cancer. Inst.* 93, 597–
394 604.

395 Barthelmes, J., Perera, G., Hombach, J., Dünnhaupt, S., Bernkop-Schnürch, A., 2011. Development of
396 a mucoadhesive nanoparticulate drug delivery system for a targeted drug release in the bladder.
397 *Int. J. Pharm.* 416, 339–345.

398 Barthelmes, J., Dünnhaupt, S., Unterhofer, S., Perera, G., Schlocker, W., Bernkop-Schnürch, A., 2013.
399 Thiolated particles as effective intravesical drug delivery systems for treatment of bladder-related
400 diseases. *Nanomedicine* 8, 65–75.

401 Berginc, K., Suljaković, S., Škalko-Basnet, N., Kristl, A., 2014. Mucoadhesive liposomes as new
402 formulation for vaginal delivery of curcumin. *Eur. J. Pharm. Biopharm.* 87, 40–46.

403 Bernkop-Schnürch, A., 2005. Thiomers: The next generation of mucoadhesive polymers. *Adv. Drug*
404 *Deliv. Rev.* 57, 1569–1582.

405 Brannigan, R.P., Khutoryanskiy, V.V., 2017. Synthesis and evaluation of mucoadhesive acryloyl-
406 quaternized PDMAEMA nanogels for ocular drug delivery. *Colloids Surfaces B Biointerfaces*
407 155, 538–543.

408 Burjak, M., Bogataj, M., Velnar, M., Grabnar, I., Mrhar, A., 2001. The study of drug release from
409 microspheres adhered on pig vesical mucosa. *Int. J. Pharm.* 224, 123–130.

410 Chuang, Y.C., Tyagi, P., Huang, C.C., Yoshimura, N., Wu, M., Kaufman, J., Chancellor, M.B., 2009.
411 Urodynamic and immunohistochemical evaluation of intravesical botulinum toxin A delivery
412 using liposomes. *J. Urol.* 182, 786–792.

413 Chuang, Y.C., Kaufmann, J.H., Chancellor, D.D., Chancellor, M.B., Kuo, H.C., 2014. Bladder
414 instillation of liposome encapsulated onabotulinumtoxin A improves overactive bladder symptoms:
415 A prospective, multicenter, double-blind, randomized trial. *J. Urol.* 192, 1743–1749.

416 Chutipongtanate, S., Thongboonkerd, V., 2010. Systematic comparisons of artificial urine formulas for
417 in vitro cellular study. *Anal. Biochem.* 402, 110–112.

418 Chen, D., Song, D., Wientjes, M.G., Au J. L-S., 2003. Effect of Dimethyl Sulfoxide on Bladder Tissue
419 Penetration of Intravesical Paclitaxel. *Clinical Cancer Research* 9, 363–369.

420 Cook, M.T., Tzortzis, G., Charalampopoulos, D., Khutoryanskiy, V.V., 2011. Production and
421 evaluation of dry alginate-chitosan microcapsules as an enteric delivery vehicle for probiotic
422 bacteria. *Biomacromolecules* 12, 2834–2840.

423 Cook, M.T., Schmidt, Lee, S.A.E., Samprasit, W., Opanasopit, P., Khutoryanskiy, V.V., 2015.
424 Synthesis of mucoadhesive thiol-bearing microgels from 2-(acetylthio)ethylacrylate and 2-

425 hydroxyethylmethacrylate: novel drug delivery systems for chemotherapeutic agents to the
426 bladder. *J. Mater. Chem. B*, 2015, 3, 6599-6604.

427 Davidovich-Pinhas, M., Harari, O., Bianco-Peled, H., 2009. Evaluating the mucoadhesive properties of
428 drug delivery systems based on hydrated thiolated alginate. *J. Control. Release* 136, 38–44.

429 Davidovich-Pinhas, M., Bianco-Peled, H., 2011. Physical and structural characteristics of acrylated
430 poly(ethylene glycol)-alginate conjugates. *Acta Biomater.* 7, 2817–2825.

431 Davidovich-Pinhas, M., Bianco-Peled, H., 2014. Methods to study mucoadhesive dosage forms, in:
432 Khutoryanskiy, V.V. (Ed.), *Mucoadhesive Materials and Drug Delivery Systems*. John Wiley &
433 Sons, Ltd, pp. 175–196.

434 Frederik, P.M., Hubert, D.H.W., 2005. Cryoelectron microscopy of liposomes. *Methods Enzymol.* 391,
435 431–448.

436 GuhaSarkar, S., Banerjee, R., 2010. Intravesical drug delivery: Challenges, current status, opportunities
437 and novel strategies. *J. Control. Release* 148, 147–159.

438 Harris, J.R., 1986. A comparative negative staining study of aqueous suspensions of sphingomyelin.
439 *Micron Microsc. Acta* 17, 175–200.

440 Hombach, J., Bernkop-Schnürch, A., 2010. Mucoadhesive drug delivery systems, in: Schäfer-Korting,
441 M. (Ed.), *Drug Delivery*. Springer Berlin Heidelberg, Berlin, Heidelberg, pp. 251–266.

442 Irmukhametova, G.S., Mun, G.A., Khutoryanskiy, V.V., 2011. Thiolated mucoadhesive and PEGylated
443 nonmucoadhesive organosilica nanoparticles from 3-mercaptopropyltrimethoxysilane. *Langmuir*
444 27, 9551–9556.

445 Kandzija, N., Khutoryanskiy, V.V., 2017. Delivery of riboflavin-5'-monophosphate into the cornea:
446 can liposomes provide any enhancement effects? *J. Pharm. Sci.* 106, 3041–3049.

447 Kawamorita, N., Yoshikawa, S., Kashyap, M., Tyagi, P., Arai, Y., Chancellor, M.B., Yoshimura, N.,
448 2016. Liposome Based Intravesical Therapy Targeting Nerve Growth Factor Ameliorates Bladder
449 Hypersensitivity in Rats with Experimental Colitis. *J. Urol.* 195, 1920–1926.

450 Khutoryanskiy, V.V., 2011. Advances in mucoadhesion and mucoadhesive polymers. *Macromol.*
451 *Biosci.* 11, 748–764.

452 Kim, K., Kim, K., Ryu, J.H., Lee, H., 2015. Chitosan-catechol: A polymer with long-lasting
453 mucoadhesive properties. *Biomaterials* 52, 161–170.

454 Kolawole, O.M., Lau, W.M., Mostafid, H., Khutoryanskiy, V.V., 2017. Advances in intravesical drug
455 delivery systems to treat bladder cancer. *Int. J. Pharm.* 532, 105–117.

456 Kulkarni, S.B., Betageri, G. V, Singh, M., 1995. Factors affecting microencapsulation of drugs in
457 liposomes. *J. Microencapsul.* 12, 229–246.

458 Malmström, P.U., 2003. Intravesical therapy of superficial bladder cancer. *Crit. Rev. Oncol. Hematol.*
459 47, 109–126.

460 Mansfield, E.D.H., de la Rosa, V.R., Kowalczyk, R.M., Grillo, I., Hoogenboom, R., Sillence, K., Hole,
461 P., Williams, A.C., Khutoryanskiy, V.V., 2016. Side chain variations radically alter the diffusion
462 of poly(2-alkyl-2-oxazoline) functionalised nanoparticles through a mucosal barrier. *Biomater.*
463 *Sci.* 35, 583–592.

464 Mun, E.A., Morrison, P.W.J., Williams, A.C., Khutoryanskiy, V.V., 2014. On the barrier properties of
465 the cornea: A microscopy study of the penetration of fluorescently labeled nanoparticles,
466 polymers, and sodium fluorescein. *Mol. Pharm.* 11, 3556–3564.

467 Mun, E.A., Williams, A.C., Khutoryanskiy, V.V., 2016. Adhesion of thiolated silica nanoparticles to
468 urinary bladder mucosa: Effects of PEGylation, thiol content and particle size. *Int. J. Pharm.* 512,
469 32–38.

470 Nii, T., Ishii, F., 2005. Encapsulation efficiency of water-soluble and insoluble drugs in liposomes
471 prepared by the microencapsulation vesicle method. *Int. J. Pharm.* 298, 198–205.

472 Oswald, M., Geissler, S., Goepferich, A., 2016. Determination of the activity of maleimide-
473 functionalized phospholipids during preparation of liposomes. *Int. J. Pharm.* 514, 93-102.

474 Rangsimawong, W., Opanasopit, P., Rojanarata, T., Duangjit, S., Ngawhirunpat, T., 2016. Skin
475 transport of hydrophilic compound-loaded PEGylated lipid nanocarriers: Comparative study of
476 liposomes, niosomes, and solid lipid nanoparticles. *Biol. Pharm. Bull.* 39, 1254–1262.

477 Robenek, H., Severs, N.J., 2008. Recent advances in freeze-fracture electron microscopy: the replica
478 immunolabeling technique. *Biol. Proced. Online* 10, 9–19.

479 Sasaki, H., Karasawa, K., Hironaka, K., Tahara, K., Tozuka, Y., Takeuchi, H., 2013. Retinal drug
480 delivery using eyedrop preparations of poly-l-lysine-modified liposomes. *Eur. J. Pharm.*
481 *Biopharm.* 83, 364–369.

482 Shtenberg, Y., Goldfeder, M., Schroeder, A., Bianco-Peled, H., 2017. Alginate modified with
483 maleimide-terminated PEG as drug carriers with enhanced mucoadhesion. *Carbohydr. Polym.*
484 175, 337-346.

485 Sou, K., 2011. Electrostatics of carboxylated anionic vesicles for improving entrapment capacity.
486 *Chem. Phys. Lipids* 164, 211–215.

487 Stewart, B.W., Wild, C.P., 2014. World cancer report 2014, International Agency for Research on
488 Cancer.

489 Storha, A., Mun, E.A., Khutoryanskiy, V.V., 2013. Synthesis of thiolated and acrylated nanoparticles
490 using thiol-ene click chemistry: towards novel mucoadhesive materials for drug delivery. *RSC*

491 Adv. 3, 12275–12279.

492 Symonds, B., Lindsay, C.I., Thomson, N.R., Khutoryanskiy, V.V., 2016. Chitosan as a rainfastness
493 adjuvant for agrochemicals. RSC Adv. 6, 102206–102213.

494 Thompson, R.F., Walker, M., Siebert, C.A., Muench, S.P., Ranson, N.A., 2016. An introduction to
495 sample preparation and imaging by cryo-electron microscopy for structural biology. Methods 100,
496 3–15.

497 Tonglairoum, P., Brannigan, R.P., Opanasopit, P., Khutoryanskiy, V.V., 2016. Maleimide-bearing
498 nanogels as novel mucoadhesive materials for drug delivery. J. Mater. Chem. B 4, 6581–6587.

499 Torre, L.A., Bray, F., Siegel, R.L., Ferlay, J., Lortet-tieulent, J., Jemal, A., 2015. Global Cancer
500 Statistics, 2012. CA a cancer J. Clin. 65, 87–108.

501 Tyagi, P., Wu, P.C., Chancellor, M., Yoshimura, N., Huang, L., 2006. Recent advances in intravesical
502 drug/gene delivery. Mol. Pharm. 3, 369–379.

503 Verma, D.D., Verma, S., Blume, G., Fahr, A., 2003. Particle size of liposomes influences dermal
504 delivery of substances into skin. Int. J. Pharm. 258, 141–151.

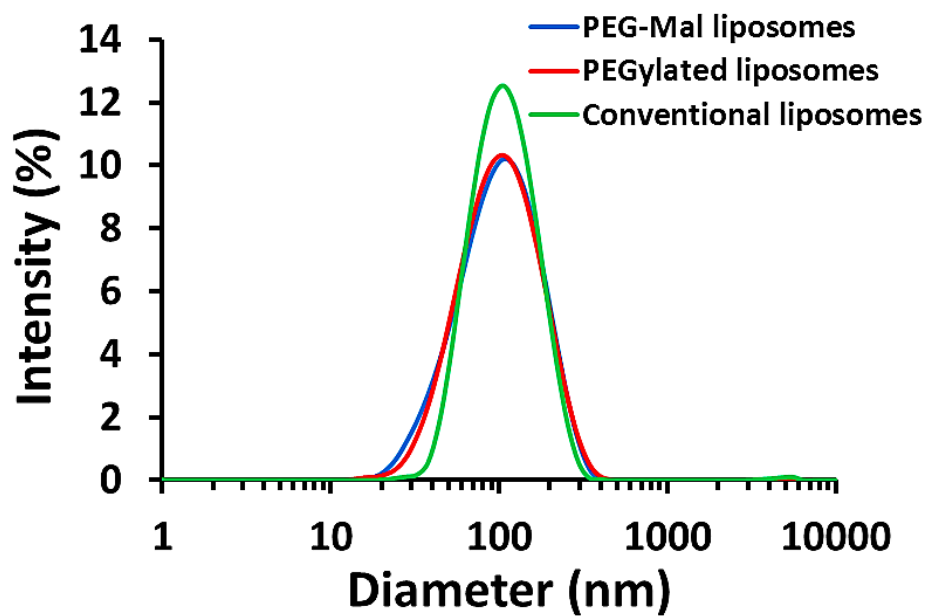
505 Wang, Y.Y., Lai, S.K., Suk, J.S., Pace, A., Cone, R., Hanes, J., 2008. Addressing the PEG
506 mucoadhesivity paradox to engineer nanoparticles that “slip” through the human mucus barrier.
507 Angew. Chemie - Int. Ed. 47, 9726–9729.

508

509

510 **Figures and legends**

511



512

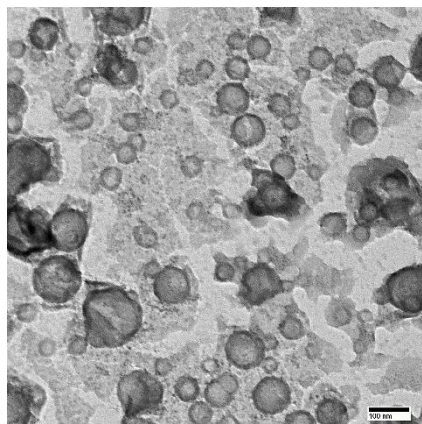
513

514 **Figure 1**

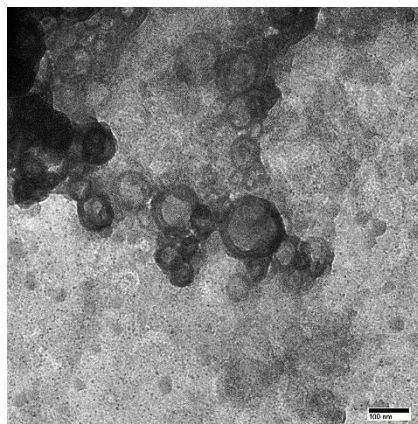
515

516

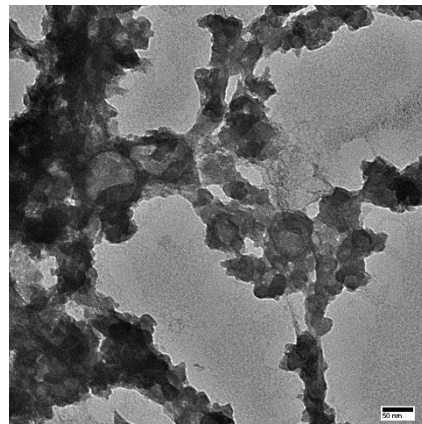
517



A



B



C

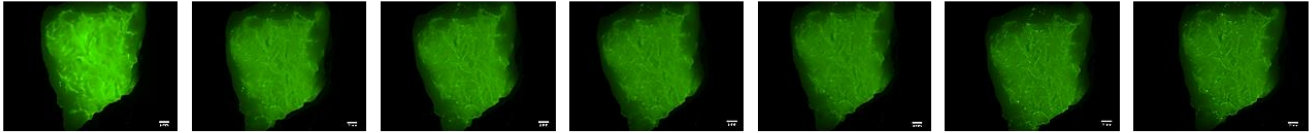
518

519 **Figure 2**

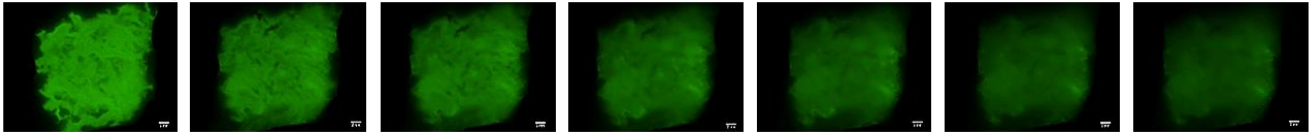
520

521

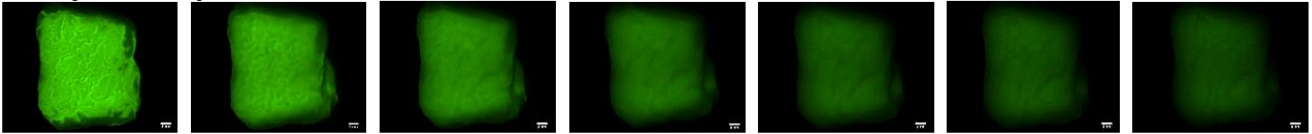
FITC-chitosan



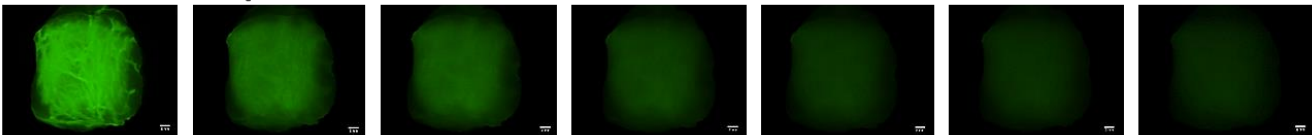
PEG-Mal liposomes



PEGylated liposomes



Conventional liposomes



FITC-dextran



0 10 20 40 60 80 100 mL



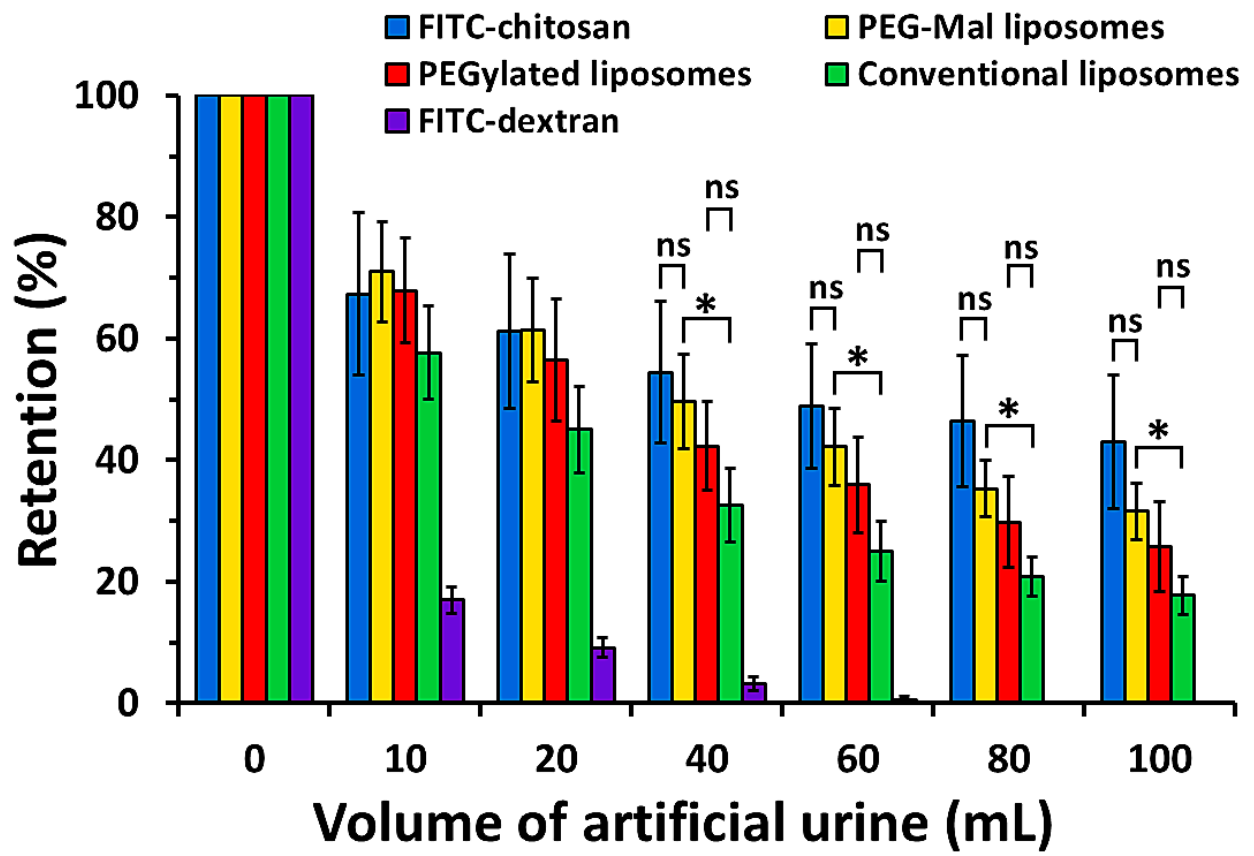
522

523

524 Figure 3

525

526



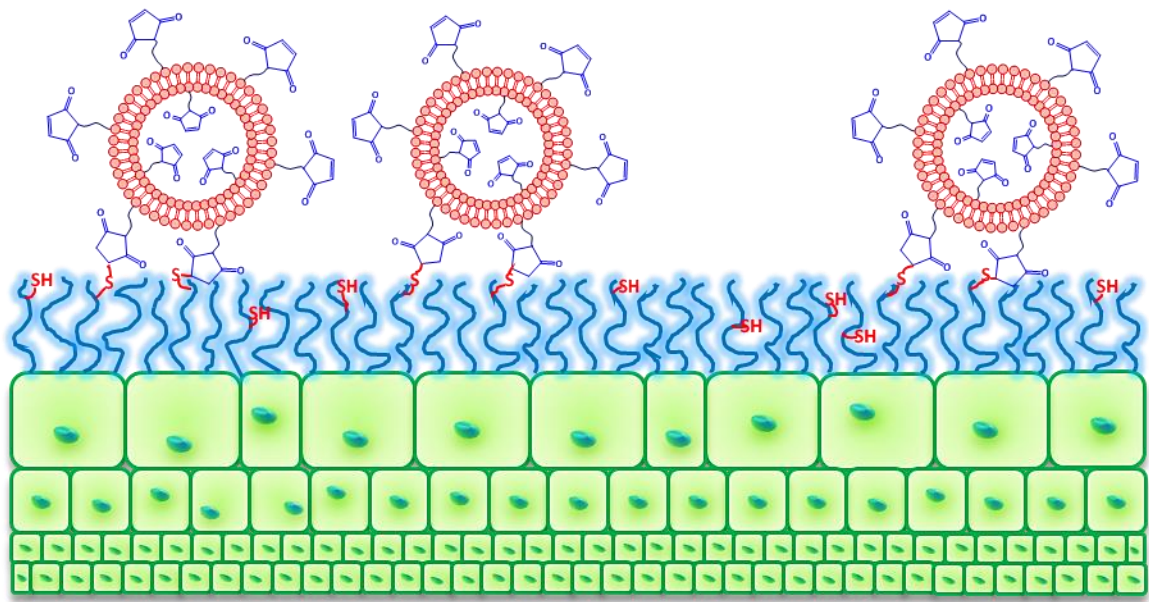
527

528

529 Figure 4

530

531



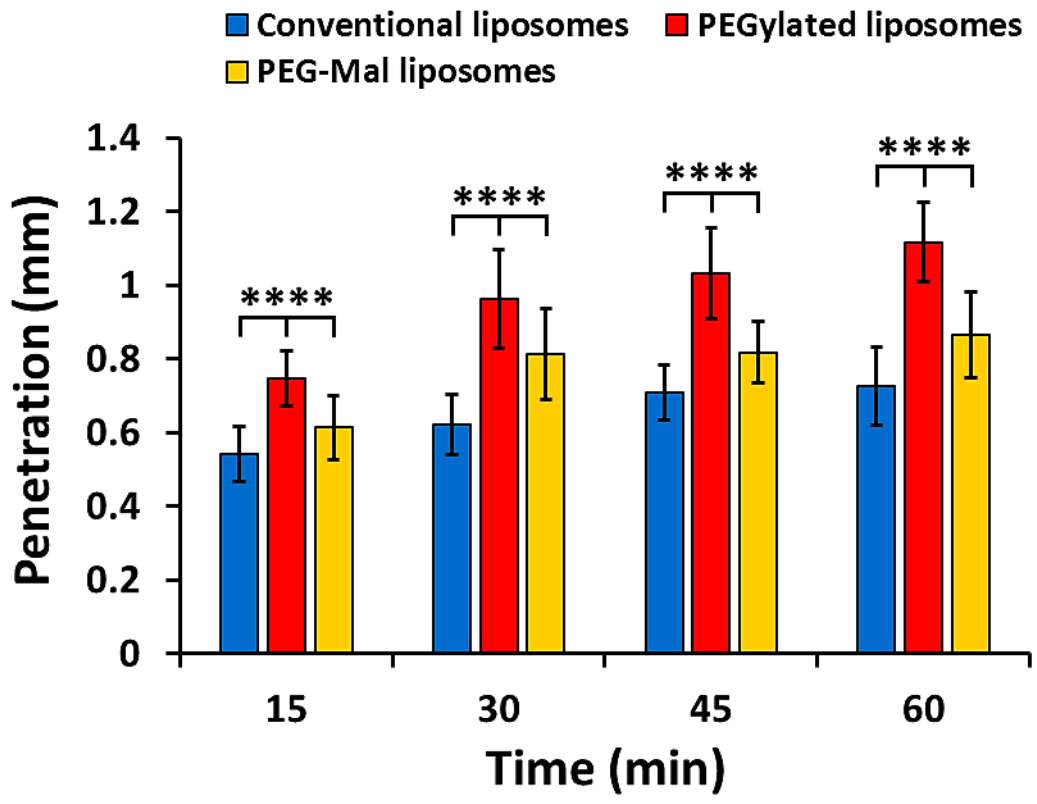
532

533

534 Figure 5

535

536



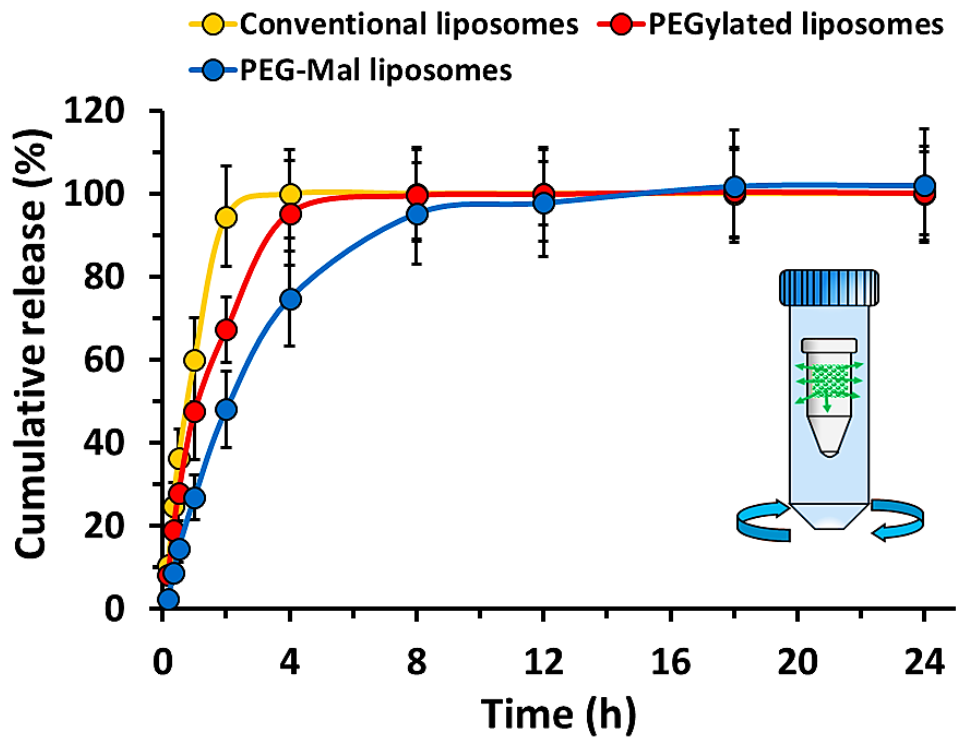
537

538

539 Figure 6

540

541



542

543

544 Figure 7

545

546

547 Figure 1 Size distribution of conventional, PEGylated and PEG-Mal liposomes as determined by DLS
548
549 Figure 2 TEM micrographs of conventional (A), PEGylated (B) and PEG-Mal liposomes (C). Scale
550 bars are 100 nm for (A) and (B), and 50 nm for (C)
551
552 Figure 3 Exemplar fluorescence images showing retention of FITC-chitosan, PEGylated, PEG-Mal
553 liposomes, conventional liposomes and FITC-dextran on porcine urinary bladder mucosa washed with
554 different volumes of AU. Scale bars are 2 μ m
555
556 Figure 4 Percentage retention of conventional liposomes, PEGylated, PEG-Mal liposomes, FITC-
557 chitosan and FITC-dextran on porcine urinary bladder mucosa after irrigating with different volumes of
558 AU. Data are expressed as mean \pm standard deviation (n = 3). *Statistically significant difference (p <
559 0.05)
560
561 Figure 5 Proposed mechanism of bonding between maleimide-functionalised liposomes and mucosal
562 surfaces
563
564 Figure 6 Penetration of the conventional, PEGylated, PEG-Mal liposomes over 60 mins. Values
565 represent the mean penetration across 10 separate porcine urinary bladder tissue sections \pm standard
566 deviation
567
568 Figure 7 Cumulative release profile of fluorescein sodium from liposomal formulations. Data expressed
569 as mean standard deviation (n =3). Insert shows the experimental set-up used in the release studies
570
571

572 Table 1 The composition (%) of lipid nanocarrier formulations.

Liposome formulations	PC	CHO	MPEG ₂₀₀₀ -DSPE	PEG ₂₀₀₀ -DSPE-Mal	NaFI
Conventional	0.773	0.077	-	-	0.2
PEGylated	0.773	0.077	0.075	-	0.2
PEG-Mal	0.773	0.077	-	0.075	0.2

PC – Soybean L-alpha-phosphatidylcholine; CHO – Cholesterol; MPEG₂₀₀₀-DSPE – [N-(carbonyl-methoxypolyethylene glycol-2000)-1,2-distearoyl-sn-glycero-3-phosphoethanol-amine, sodium salt]; PEG₂₀₀₀-DSPE-Mal – 1,2-distearoyl-sn-glycero-3-phosphoethanolamine-N-[maleimide(polyethylene glycol)-2000] ammonium salt; NaFI – Fluorescein sodium salt

573

574

575

576 Table 2 Physicochemical characteristics of conventional, PEGylated and PEG-Mal liposomes.

Liposome formulations	Mean diameter, nm	PDI	Zeta potential, mV	%EE	%LC	WO ₅₀ , mL
Conventional	97 ± 1	0.145	-53 ± 1	53 ± 6	12 ± 1	15
PEGylated	85 ± 1	0.217	-32 ± 2	27 ± 2	6 ± 1	24
PEG-Mal	86 ± 1	0.224	-37 ± 1	25 ± 2	5 ± 1	48

WO₅₀, volume of AU required to wash out 50% of liquid formulation. Results are given as mean ± standard deviation (n = 3)

577